

# Applications of reinforcement particles in the fabrication of Aluminium Metal Matrix Composites by Friction Stir Processing - A Review

Karthik Adiga<sup>\*</sup> , Mervin A. Herbert, Shrikantha S. Rao, and Arunkumar Shettigar 

Department of Mechanical Engineering, National Institute of Technology Karnataka, Surathkal, India

Received: 5 May 2022 / Accepted: 16 August 2022

**Abstract.** Composite materials possess advantages like high strength and stiffness with low density and prove their essentiality in the aviation sector. Aluminium metal matrix composites (AMMC) find applications in automotive, aircraft, and marine industries due to their high specific strength, superior wear resistance, and lower thermal expansion. The fabrication of composites using the liquid phase at high temperature leads to the formation of intermetallics and unwanted phases. Friction Stir Processing (FSP) is a novel technique of composite fabrication, with temperature below the melting point of the matrix, achieving good grain refinement. Many researchers reported enhancement of mechanical, microstructure, and tribological properties of AMMC produced by the FSP route. The FSP parameters such as tool rotational speed, tool traverse speeds are found to be having greater impact on uniform dispersion of particles. It is observed that the properties such as tensile strength, hardness, wear and corrosion resistance, are altered by the FSP processes, and the scale of the alterations is influenced significantly by the processing and tool parameters. The strengthening mechanisms responsible for such alterations are discussed in this paper. Advanced engineering materials like shape memory alloys, high entropy alloys, MAX phase materials and intermetallics as reinforcement material are also discussed. Challenges and opportunities in FSP to manufacture AMMC are summarized, providing great benefit to researchers working on FSP technique.

**Keywords:** Friction stir processing / aluminium metal matrix composites / reinforcement particles / solid state processing / structure property

## 1 Introduction

Industries like aircraft, automobile, marine, etc. demand lightweight materials that help to reduce fuel consumption and improve efficiency. The conventional alloys which have lesser weight density, good strength to weight ratio and high corrosive resistance are used for different applications. However, the strength and stiffness of these alloys are not good enough to use in structural applications. This leads to the production of composites, by physically and/or chemically combining two or more engineering constituents using the processing technique [1]. The composites prepared by incorporating reinforcement particles are superior in mechanical, metallurgical, and tribological properties compared to the base alloy. The reinforcement of particles into the metal matrix is of three types, namely, metal matrix composites, surface composite and functionally graded composites. In Metal Matrix Composites

(MMC), particles are reinforced throughout the whole volume, and in Functionally Graded Composites (FGC), reinforcements are incorporated as gradual transitions in the volume percentage. When reinforcement of particles is limited at surface level, surface composites are formed [2]. The composites are fabricated by dispersing reinforcement particles in a metal matrix using techniques like powder metallurgy, spray deposition, laser treatment and casting, etc. The aforementioned techniques are liquid phase processing at high temperatures, which form detrimental phases and intermetallic compounds [3].

AMMC have gained significant attention in the areas like aerospace, electrical, aviation, automotive, military and thermal, etc. because of their high strength to weight ratio, good corrosion and wear resistance, high thermal and electrical conductivity, and high specific stiffness and strength [4]. Authors [5,6] discussed the different fabrication methods of aluminium matrix composites and their role in enhancing mechanical and wear properties. The traditional AMMC fabrication methods result in microstructural defects, cracks, segregation, porosity, and

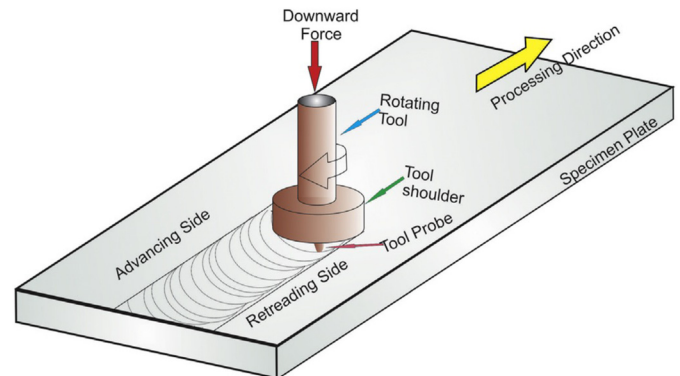
\* e-mail: [karth242@gmail.com](mailto:karth242@gmail.com)

**Table 1.** Industrial application of AMMC.

Si. No	Industry	Applications	Reasons
1	Automobile	Pistons, connecting rods, brake rotors, current collectors, A/C pump bracket, engine blocks, propeller shafts, brake disc	Higher damping, self-cleaning, self-healing capability, good corrosion and wear resistance, less noise
2	Aerospace and aircraft	Fuselage, wings and supporting structure in airlines, landing gear parts, vertical tails and brakes, military aircrafts	High strength to weight ratio, lower fuel consumption, lower thermal coefficient of expansion
3	Rail transport	Railway cars	Better fuel efficiency, higher load carrying capacities, Durability
4	Marine transport	High speeds to boats at higher fuel efficiency	reduced maintenance costs
5	Off-shore applications	Offshore platforms and seawalls	Greater strength, low cost
6	Building and construction	Supporting structure in building materials	Greater strength and stiffness
7	Packaging and Containerization	Beverage bottles and cans, food containers, industrial foils	
8	Sports and recreation	Sports goods	Greater strength and lightweight
9	Electrical transmission	Electrical transmission	Lightweight, higher corrosion resistance, high efficiency in conduction

clustering of particles. Ceramic particles like silicon carbide, boron carbide, titanium carbide, titanium dioxide, and aluminium oxide, etc. are used as reinforcement to produce metal matrix composites. The reinforcement material should be very hard and robust, light in weight and must have higher strength to weight ratio than matrix materials. Lower fuel consumption, lower airborne emission and less noise are the key benefits of aluminium based composites in transportation sector. Table 1 lists the industrial applications of AMMC [7].

Friction stir processing is a variant of the Friction Stir Welding (FSW) process, developed by Mishra et al. [8]. FSP being a solid phase processing technique, limits the problems of liquid-phase processing techniques. The material processing applications such as grain refinement, microstructural homogeneity, surface modification, super-plasticity, coating, weld repair, and fabrication of surface composites are performed by FSP [9]. The working principle of FSP is similar to FSW except that FSP is performed on a single plate, while FSW is used to join the materials. In FSP, a non-consumable rotating tool with a specially designed probe is plunged into the specimen until tool shoulder touches the workpiece surface and traverses in the desired direction [10]. The interaction between the rotating tool and specimen generates sufficient heat to soften the workpiece material [11]. The probe stirs the softened material and fills the cavity at the rear of the tool. [12]. As the tool traverses in the desired direction, the processed region will form behind the tool owing to the forging action of materials below the tool shoulder. Significant microstructure refinement in the processed zone results from severe plastic deformation of material

**Fig. 1.** Schematic illustration of FSP [15].

flows around the tool. The recent advances in FSW/FSP over the years have been critically reviewed by [13]. The state-of-the-art of friction stir processing as a solid state grain refinement technique under microstructure evolution and property enhancement is discussed by Patel et al. [14]. Figure 1 shows the schematic representation of FSP process.

## 2 Composite fabrication by friction stir processing (FSP)

Friction Stir Processing (FSP) as a solid-state processing method has demonstrated significant advantages over the conventional composite fabrication techniques with less or no interfacial reaction. The conventional techniques form an interfacial reaction between the metal matrix and

**Table 2.** FSP parameters involved in composite fabrication.

Machine Variables	Tool design variables	Reinforcement variables	Material Properties	Other variants
Tool rotational speed	Shoulder ↗ Diameter ↘ Profile	Particle size	Mechanical	Number of passes
Tool traveling speed		Reinforcement strategy	Thermal	Direction between successive passes
Tool tilt angle	Pin ↗ Diameter → Profile ↘ Length	Types (mono and hybrid)		
Axial force		Volume fraction of particles		
Plunge depth				

reinforcement, which deteriorate the composite properties further. The reinforcement particles are filled in pre-machined grooves or holes produced on the surface of the matrix. The strategies to incorporate reinforcement particles into the metallic matrix are discussed in [16,17]. The groove filling and hole filling methods are very widely used reinforcement strategies. The grooves or holes are then processed with pin less tool to prevent the scattering of particles. The FSP tool with suitable pin geometry and rotational speed is then plunged into the workpiece till the tool shoulder touches the matrix surface. The FSP parameters involved in composite fabrication are listed in Table 2. The heat generated due to the friction between the rotating tool shoulder and workpiece plasticizes the matrix metal. After providing a certain dwell time post plunging, traverse speed is provided to the tool. The tool traverse movement causes the transportation of plasticized matrix material from the advancing side to the retreating side. The combined action of rotational and traverse speed helps to mix the reinforcement particles with the workpiece and thus formation of composites.

The surface composites or composite fabrication using FSP can be accomplished via two ways, i.e., ex-situ and in-situ. In ex-situ fabrication method, the reinforcement particles are added to base matrix externally and FSP is performed. On the other hand, in in-situ type the reinforcement becomes innate during composite synthesis which needs completion of certain reactions. Mishra et al. [18] explored the use of the FSP technique in the fabrication of the Al5083 surface composite by reinforcing the silicon carbide particle. In this pioneered work, the authors applied SiC powder into the surface of plates and processed them with FSP. The novel technique proved worth by successfully distributing SiC particles in the aluminium matrix and forming a fine microstructure. This work paved the way for numerous studies to develop surface composites by incorporating reinforcement particles via FSP. The studies revealed that particles like boron carbide [19,20], silicon

carbide [21–23], titanium carbide [24], tungsten carbide [25], aluminium oxide [26], titanium dioxide [27] and titanium diboride [28] etc. can also mix well with the aluminium matrix during FSP and greatly influence the microstructural and mechanical properties. Sharma et al. [15] discussed the different FSP process variable involved in surface composite fabrication. This detail review work also reported on the strengthening mechanism and strengthening model of friction stir processed surface composite. The review article by Bharti et al. [29] discussed the FSP process parameters like tool geometry, tool speed, reinforcement particle, number of passes and their effect on material properties like corrosion, hardness, wear, tensile strength. The other studies [3,17] are also explored the strategies and technological aspect of FSP in fabricating surface composites. However, there is no or very few literatures are available about exclusive study of various reinforcement particles used in composite fabrication by FSP.

This review article aimed to discuss different reinforcement particles used in AMMC fabrication via FSP. The reinforcement particles and their role in property enhancement are elucidated. An attempt has been made to emphasize the previous work carried out on the processing of aluminium based composites by Friction Stir processing using different reinforcements.

### 3 Reinforcements

The reinforcement must be hard, robust and light in weight. The reinforcement is used to enhance the material properties such as wear resistance, stiffness, corrosion resistance, strength, and young's modulus. The mechanical properties of reinforcement are stronger than the matrix materials [30].

Ceramic materials are non-metallic and inorganic materials. When the hard-ceramic particles are reinforced in the aluminium matrix, their strength, young's modulus and wear resistance, etc. increases. Ceramics are classified

as oxides, carbides, nitrides and borides. The Reinforcement Particles (RPs) that are used to fabricate surface composites are boron carbide ( $B_4C$ ) [31], silicon carbide (SiC) [32], titanium carbide (TiC) [24], titanium dioxide ( $TiO_2$ ), aluminium oxide ( $Al_2O_3$ ) [33], Titanium diboride ( $TiB_2$ ) [34], and Zirconium diboride ( $ZrB_2$ ).

### 3.1 Boron carbide

Boron carbide ( $B_4C$ ) is a popular reinforcement that has a density of  $2.52\text{ g/cm}^3$  and a melting point of  $2763\text{ }^\circ\text{C}$ . Boron carbide is also characterized by extreme hardness ( $2800\text{ kg/mm}^2$ ), good nuclear properties and good chemical resistance. This makes the boron carbide to be used in the nuclear power plant as neutron radiation absorbent, shielding and control rods. Al/ $B_4C$  composites are suitable for brake pads, radioactivity containment vessels and frames of bicycles, etc. The use of friction stir processing to fabricate Al/ $B_4C$  is a new technique and many works are reported on the same. The particles are encased in and flow along with the plastic metal during the FSP. Zhao et al. [31] fabricated the AA6061/ $B_4C$  surface composites by using FSP. Upon investigation, it was found that an increase in FSP passes leads to a homogeneous distribution of  $B_4C$  particles in the weld zone, which improved the wear resistance and microhardness of composites (98 HV) as compared to the base matrix. Due to the complexity of material flow, the multiple passes of FSP are essential to reduce the size of particle clusters, uniform distribution of particles, easy dispersion and avoidance of particle agglomeration. The particle agglomeration is also visible in the sample processed at too low tool rotational speed, too high tool traverse speed and coarse particles. Rana et al. [20,35] produced the AA7075/ $B_4C$  surface composites (SCs) by evaluating the effect of particle size, reversal of tool direction between passes, and tool rotational speeds. Superior distribution of  $B_4C$  particles was found at reduced particle size, reversing the stirring tool direction and lower rotational speed. The FSP multipass with a change in stirring direction after each pass ensures uniform material and powder movement on both the advancing and retreating sides. As a result, the sample has less powder particle agglomeration and more homogeneous distribution. Because of the stronger particle-substrate bond, the fine size of powder particles also leads to homogeneous distribution. The approach of change in stirring direction after each pass is also found to reduce wear in the processed aluminium surface composites, as reported by Mehta et al. [36]. The incorporation of  $B_4C$  reinforcement particles by FSP into AA6061 alloy was found to reduce friction and wear rate as reported by [37]. The hard boron carbide particles act as a load bearing component and reduce the direct load contact between the composite surface and disk. AA 6061/ $B_4C$  composite showed less friction ( $\mu \sim 0.4$ ) and a 75 times reduction in wear. Komarasamy et al. [38] achieved the homogeneous distribution of particles with good interfacial bonding in FSP fabricated Al5024/ $B_4C$  SCs. The orowan strengthening and grain strengthening mechanism are the main reasons for the increase in hardness of surface composites. Akbari et al. [39] optimized the microstructural and mechanical properties of  $B_4C$  reinforced A356 composites produced by FSP using an artificial neural network and

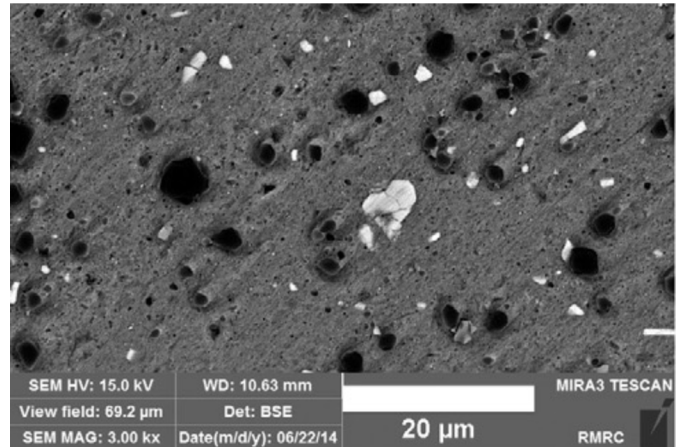


Fig. 2. SEM micrographs of AA6063- $B_4C$  surface composite [40].

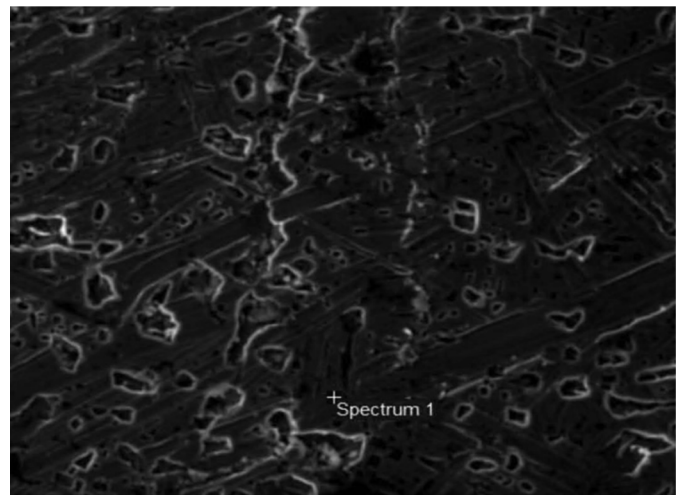


Fig. 3. SEM Micrograph of grains after friction stir processing AA1050/TiC composites at 1200 rpm and 300 mm/min [44].

non-dominated sorting genetic algorithm-II (NSGA-II). The combination of a higher ratio of tool rotational speed to traverse speed and threaded pin profile cause better particle distribution and fine Si elements. Figure 2 shows the SEM micrographs of A6063- $B_4C$  surface composite produced by friction stir processing.

### 3.2 Titanium carbide

Titanium carbide (TiC) is a prominent material reinforcement agent owing to high melting temperature ( $3067\text{ }^\circ\text{C}$ ), high Vickers hardness (28–35 GPa), high elastic modulus (450 GPa), good electrical conductivity ( $30 \times 10^6\text{ .S cm}^{-1}$ ) and density of  $4.91\text{ g/cc}$ . Al-TiC composites are used in aerospace, space technology and automobile industries. Thangarasu [24] fabricated AA1050/TiC surface composite by FSP and observed the homogeneous distribution of TiC particle in FSP zone and 45% increase in hardness. Akinlabi

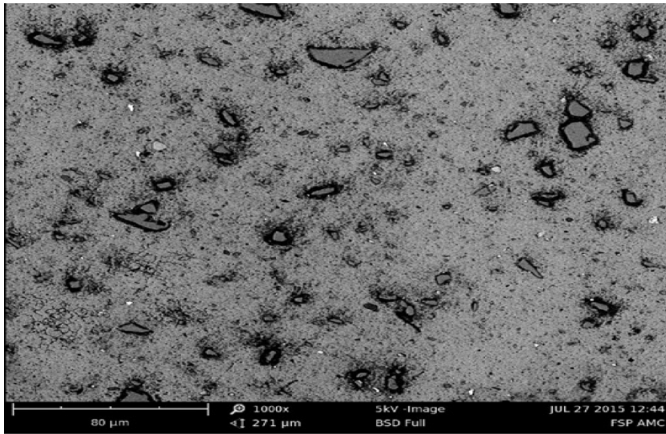


Fig. 4. SEM micrograph of AA6082 AMC containing  $\text{TiB}_2$  particles [47].

et al. [41] found the optimum process parameters to produce a surface composite with the best wear-resistant property in AA1050/TiC composites. The refined grains in AA1050/TiC composites processed at 1200 rpm and 300 mm/min is shown in Figure 3. Further, Dinaharan [42] produced aluminium matrix composites using AA6082 as a matrix, and different ceramic particles (SiC, TiC,  $\text{B}_4\text{C}$ ,  $\text{Al}_2\text{O}_3$ , and WC) are as reinforcements. AA6082/TiC Aluminium Matrix Composites (AMC) showed better hardness (120 VHN) and UTS (326 MPa). Incorporation of TiC particles influences the stir zone area, grain size of the matrix, microhardness, and wear resistance in FSP fabricated AA6082/TiC AMC [43].

### 3.3 Titanium diboride

Titanium diboride ( $\text{TiB}_2$ ) has a density of 4.52 g/cc and a melting point of 3225 °C.  $\text{TiB}_2$  finds application in armor components, cutting tools, and crucibles due to high density, high elastic modulus (510–575 GPa) and high compressive strength. Narimani et al. [28] enhanced the tensile strength up to 70% by incorporating mechanical alloying  $\text{TiB}_2$ -Al particles into the AA6063 matrix using FSP. Many works were reported on friction stir processing of Al- $\text{TiB}_2$  in situ composites [34,45,46]. Figure 4 illustrates the SEM micrographs of AA6082/ $\text{TiB}_2$  composites.

### 3.4 Aluminium oxide

Aluminium oxide ( $\text{Al}_2\text{O}_3$ ) is an important reinforcement that has a density of 4.09 g/cc and a melting point of 2072 °C. Due to the high strength to weight ratio, good castability, and good tribological properties, Al/ $\text{Al}_2\text{O}_3$  metal matrix composites are used in the automotive, aircraft, and aerospace fields. Shafiei-Zarghani et al. [26,48] studied the effect of the number of passes on microstructure and mechanical properties of Al6082/ $\text{Al}_2\text{O}_3$  nanocomposites fabricated by FSP. The obtained results indicated an increase in the number of FSP passes caused a more uniform distribution of nano alumina particles, a decrease in

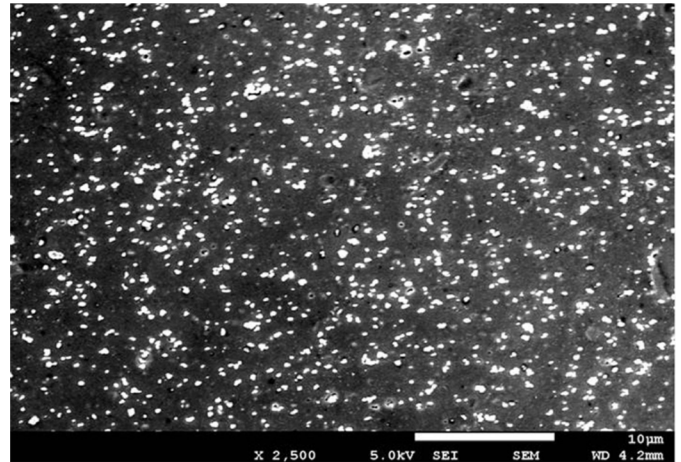
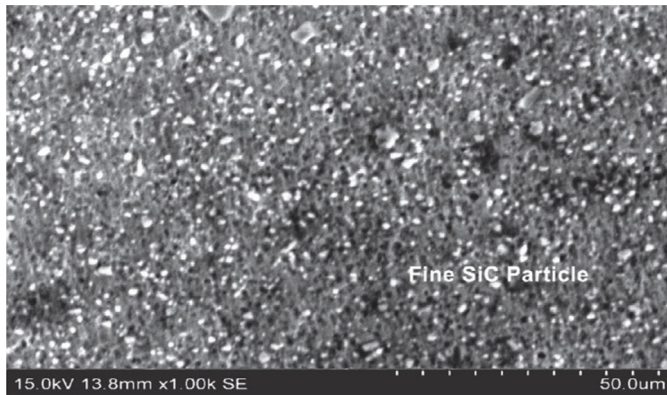


Fig. 5. FESEM Micrographs of FSPed Al- $\text{Al}_2\text{O}_3$  composites [50].

matrix grain size, better wear resistance and improved microhardness (295 HV). Authors pointed out that, in four Pass FSP (i) The pinning effect by nano  $\text{Al}_2\text{O}_3$  particle impedes the grain growth. (ii) Orowan strengthening mechanism due to the presence of nano  $\text{Al}_2\text{O}_3$  particle causes high microhardness in surface nanocomposite. (iii) Improvement in hardness causes improved wear resistance. The uniform distribution of nano  $\text{Al}_2\text{O}_3$  particles in FSPed Al- $\text{Al}_2\text{O}_3$  composite can be observed in Figure 5. Bourkhani et al. [33] investigated the distribution of alumina nanoparticles, evolution of grain structure, tensile and tribological properties in samples extracted from the top surface of the fabricated composite. The base material was AA1050 and the reinforcement was  $\text{Al}_2\text{O}_3$ . After applying the single pass FSP to fabricate AA1050/ $\text{Al}_2\text{O}_3$  nanocomposites, the authors prepared four samples of 2 mm thickness extracted from each 2 mm of the composite (0–2 mm, 2–4 mm, 4–6 mm, 6–8 mm). The same extraction method is repeated for 2 pass FSP. Further, Parumandla et al. [49] found a combination of process parameters to get defect-free conditions in Al6061/ $\text{Al}_2\text{O}_3$  nanocomposites fabricated by FSP. The author studied the effect of tool shoulder geometry, tool rotational speed and tool traverse speed on the microstructure, material flow, and mechanical properties of Al6061/ $\text{Al}_2\text{O}_3$  nanocomposites. The defect-free composite was produced using a tool with a 24 mm shoulder diameter that rotated at 1150 rpm and traversed at 15 mm/min. In defect-free conditions, superior microhardness (132 HV) was achieved, but tensile strength was reduced (172 MPa).

### 3.5 Silicon carbide

Silicon carbide (SiC) is the popular reinforcement used to fabricate AMMCs. It has a density of 3.20 g/cc and a melting point of 2700 °C. SiC reinforced Aluminum matrix composites have high wear resistance, high corrosion resistance and low thermal expansion coefficient. These composites find applications in aerospace equipment, structural materials in satellites, automotive pistons and brake discs. Many researchers have used friction stir processing technique to fabricate Al/SiC composites.



**Fig. 6.** SEM micrographs of FSPed Al/SiC composites processed at a  $D/d$  ratio of 3 [58].

Eftekharinia et al. [51] fabricated Al6061-T6/SiC surface composites by FSP and investigated the effects of pin geometry and the number of passes on macrostructure, microstructure, wear rate and microhardness. The authors discovered that (i) the material flow and mixing are enhanced by the threads on the pin. (ii) Square profile of the pin produces a finer grain size ( $3.41 \mu\text{m}$ ) in the stir zone, the highest average hardness (130 HV) and higher wear resistance. The tool pin profile affects the material flow and particle distribution. Flat pin profiles produce pulsating action in flowing materials and are also associated with eccentricity, which is the ratio between the dynamic volume swept by the tool and tool static volume. The pulsating action is measured as pulses/second (rotational speed in seconds  $\times$  number of flat faces) Elangovan et al. [52]. The threaded pin profile facilitates increased material displacement, as it moves the material in the vertical direction along with material revolution around the tool pin [53]. Tang et al. [54] found the optimum rotational tool speed (950 rpm) and tool traverse speed (60 mm/min) for uniform SiC particle distribution and refining in Al1060/SiC surface composites fabricated through FSP. An increase in FSP passes results in eliminating particle agglomeration, void in FSP fabrication of AA6063/SiC surface composites [55]. The distribution of reinforcement particles is also influenced by tool plunge depth. Rathee et al. [56] fabricated AA6061/SiC surface composites by FSP and the results showed the need for optimum tool plunge depth to get a good distribution of particles in the matrix. Lower tool plunge depths (0.10 mm, 0.15 mm, 0.2 mm) result in inadequate heat generation and cavity formation, while higher tool plunge depths (0.3 mm, 0.35 mm) result in material sticking to the tool shoulder, ejection of reinforcement particles, and so on. At a tool plunge depth of 0.25 mm, a defect-free surface composite with uniform powder distribution was discovered. Tang et al. [57] designed multi-pin tool to fabricate Al1060/SiC composites and perceived the improvement in the degree of refinement and uniformity in SiC particle distribution. Figure 6 shows the distribution of SiC particles in the LM25AA-5% SiCp metal matrix composites, friction stir processed at shoulder diameter to pin diameter ratio ( $D/d$ ) of 3.

### 3.6 Cerium oxide

Cerium oxide ( $\text{CeO}_2$ ) is another reinforcement used to fabricate metal matrix composites. It has a density of  $7.6 \text{ g/cc}$  and a melting point of  $2340 \text{ }^\circ\text{C}$ . The cathodic inhibitor property of cerium oxide prevents the reaction at the cathode, making it ideal for applications requiring increased corrosion resistance. Researchers adopted the FSP technique to fabricate AMMC, using cerium oxide as reinforcement. Amra et al. [59] produced mono and hybrid composites of Al5083/(SiC +  $\text{CeO}_2$ ) by FSP and reported that composites containing higher amounts of cerium oxide particles showed high corrosion resistance. Figure 7a shows the SEM images of uniform distribution of reinforcements in the Al5083/ $\text{CeO}_2$  composites.

### 3.7 Molybdenum disulfide

Molybdenum disulfide ( $\text{MoS}_2$ ) has a density of  $5.06 \text{ g/cc}$  and a melting point of  $2375 \text{ }^\circ\text{C}$  and is widely used as a dry lubricant because of low friction. Gupta [60] used  $\text{MoS}_2$  as reinforcement to fabricate Al1120 alloy surface composites using FSP and studied the tribological behavior of composites. Similarly, Saini et al. [61] enhanced the wear resistance by incorporating  $\text{MoS}_2$  reinforcement into the Al-17Si alloy matrix using FSP. Figure 7b shows the particle dispersion in A356/SiC/ $\text{MoS}_2$  reinforced hybrid composites.

### 3.8 Zirconium diboride

Zirconium diboride ( $\text{ZrB}_2$ ) is an ultra-high temperature ceramic, having a high melting point ( $3246 \text{ }^\circ\text{C}$ ) and a density of  $6.09 \text{ g/cc}$ . High temperature strength of zirconium diboride makes it ideal in high temperature aerospace applications. The hardness ( $>2200 \text{ HV}$ ), Young's modulus ( $450 \text{ GPa}$ ), and electrical ( $1 \text{ } 107 \text{ S/m}$ ) and thermal conductivity ( $60 \text{ W/mK}$ ) are all strong mechanical properties of  $\text{ZrB}_2$ . Zhang et al. [63,64] used multi-pass FSP to optimize the microstructural and mechanical properties of as-cast  $\text{ZrB}_2/6060\text{Al}$  composites. In fabricated composites, the four-cycle FSP helps to increase hardness (84 HV), yield strength (150 MPa), and UTS (240 MPa). The grain refinement is decided by the Zener pinning effect and the higher  $\text{ZrB}_2$  content will enhance refining efficiency. Further, Prasad et al. [65] fabricated 2 wt%  $\text{ZrB}_2/\text{AA7075}$  nanocomposite through flux assisted casting and processed through multi pass friction stir processing. The authors observed the complete breakage of  $\text{ZrB}_2$  clusters due to multipass FSP and also uniform dispersion of nanoparticles. The improvement in hardness is reported due to the pinning effect of uniformly dispersed  $\text{ZrB}_2$  nanoparticles.

### 3.9 Titanium dioxide

Titanium dioxide ( $\text{TiO}_2$ ) is an important reinforcement used in AMC fabrication. It has a density of  $4.05 \text{ g/cc}$  and a melting point of  $2103 \text{ }^\circ\text{C}$ . Researchers used the friction stir processing technique to fabricate Aluminium/  $\text{TiO}_2$

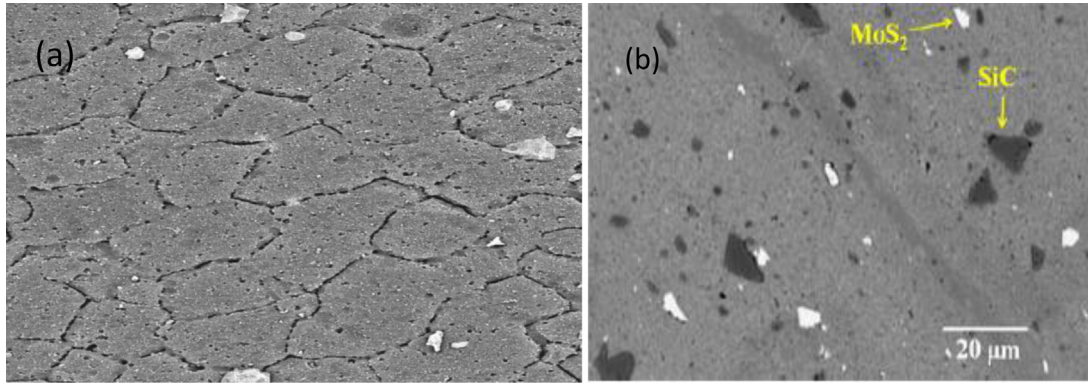


**Fig. 7.** (a) SEM images of uniform distribution of reinforcements in the Al5083/CeO<sub>2</sub> composites [59]. (b) Particle dispersion in A356/SiC/MoS<sub>2</sub> reinforced hybrid composites [62].

composites. Mathur et al. [66] considered groove width along with rotational speed and processing speed as variable parameters during FSP fabrication of AA5052/TiO<sub>2</sub> composites. The microstructural and mechanical properties are successfully enhanced in composites as compared to the base matrix. The reinforcement particles are incorporated into a groove machined on the surface of the metal matrix plate and the two are mixed when FSP is applied. The groove dimensions are important to decide the volume fraction of the reinforcement particles in the composites. The theoretical volume fraction of reinforcement particles is calculated according to equations (1)–(3) [67]. Khodabakhshi et al. [68] produced AA5052-TiO<sub>2</sub> nanocomposite using reactive friction stir processing method. The term ‘reactive’ is used because the chemical reaction between the TiO<sub>2</sub> nanoparticle and the Al-Mg matrix results in the in-situ formation of MgO and Al<sub>3</sub>Ti nanoparticles. The in-situ formation of hard inclusions enhanced the mechanical characteristics. However, Kumar et al. [69] observed no such reaction products during the fabrication of Al3003-TiO<sub>2</sub> surface composite. Madhu et al. [27] noticed a formation of Al<sub>3</sub>Ti and Al<sub>2</sub>O<sub>3</sub> as the reaction of TiO<sub>2</sub> with aluminium matrix is assisted by FSP, especially during higher passes of FSP. The combined effect of grain refining and orowan strengthening resulted in a 26% increase in yield and a 44% increase in Ultimate Tensile Strength (UTS). Ahmadifard et al. [70] found tribological behavior of A356/TiO<sub>2</sub> nanocomposite is function of hardness. The effect of FSP passes on particle distribution, microstructure, microhardness and wear properties was investigated by [71]. Author fabricated AA1050/ TiO<sub>2</sub> surface composite using FSP by single pass and second pass. While single pass surface composite showed agglomeration of particles, second pass surface composites showed homogeneous microstructure, better hardness (76 HBV) and good wear resistance (wear rate of  $176.3 \times 10^{-4} \text{ mm}^3/\text{m}$ ).

$$\begin{aligned} & \text{Theoretical volume fraction} \\ &= \frac{\text{Area of the groove}}{\text{Projected area of tool pin}} \times 100 \end{aligned} \quad (1)$$

$$\text{Area of the groove} = \text{Groove width} \times \text{Groove depth} \quad (2)$$

$$\text{Projected area of tool pin} = \text{pin diameter} \times \text{pin length}. \quad (3)$$

### 3.10 Tungsten carbide

Tungsten carbide (WC) is another prominent reinforcing material used in fabrication of AMMC. The high melting point (2870 °C), extreme hardness (2242 HV) and high young’s modulus of elasticity (550 GPa) of tungsten carbide make it an attractive reinforcing material to fabricate aluminium matrix composites [25]. Additive friction stir processing was used to prepare Al5083/WC surface composites. The Additive FSP-fabricated surface composites had a higher hardness (132 HV) and wear resistance (wear volume loss  $1.54 \times 10^8 \mu\text{m}^3$ ) than the base aluminium alloy. Grain refinement during FSP was discovered to be caused by a continuous dynamic recrystallization process [72]. The authors called the process of adding other substances into the substrate processed via FSP as Additive Friction Stir Processing (AFSP), as previous works [73,74] applied the additive technique to FSP to locally change the composition and constituent phases. Heidarpour A [75] used FSP to fabricate surface composites by incorporating WC-Al<sub>2</sub>O<sub>3</sub> particles into the Al5083 matrix. The author discovered that increasing the number of FSP passes increased grain refinement and decreased grain size (11 μm), resulting in higher hardness values (101 HV) and lower wear rates (0.026 mg/m) in surface composites.

### 3.11 Carbon nanotubes

Carbon nanotubes (CNTs) are tubes made up of graphitic carbon materials with diameters measured in nanometers. CNTs are used as reinforcements for composites due to their excellent elastic modulus (1 TPA), strength (30–100 GPa), and good thermal and electrical properties. CNTs as reinforcement can produce tailorable properties. Researchers have used the FSP metalworking technique to fabricate

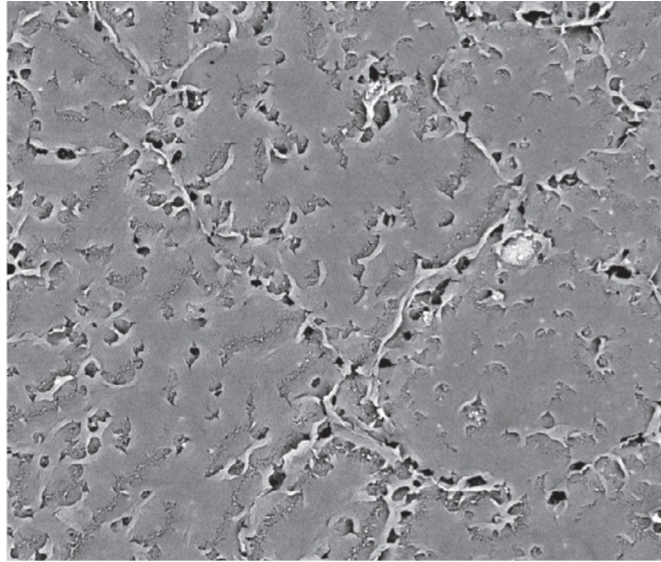


**Fig. 8.** SEM image of distribution of reinforcements after the third pass in Al5083/CNTs composites [82].

Aluminium/CNT composites along with other fabrication methods. Liu et al. [76,77] fabricated the CNT/2009Al composites by combining powder metallurgy and friction stir processing. The authors reported an increase in FSP passes shortened the CNTs and uniformly distributed the CNTs along the grain boundaries. The authors also proposed the CNT shortening and universal strength models and compared the model predictions with experimental results. Du et al. [78] have studied the effects of an increase in FSP passes on CNTs dispersion, hardness, and yield tensile strength in FSP fabricated AA6061-T6/CNTs composites. It was reported that the increasing number of passes achieved the uniform distribution of CNTs, superior hardness, refined grains structure and improved ductility of synthesized AA6061-T6/CNTs composites. Izadi et al. [79] used the FSP method to develop a higher volume percentage of CNTs reinforced composite. Two and three passes of FSP produced  $23 \pm 2.5$  and  $52 \pm 2.1$  vol.% of CNTs, respectively. The strengthening mechanisms in the composite are dependent on the size and volume fraction of reinforcement particles in the composites. Liu et al. [80] found an increase in tensile strength and microhardness with the increase of multi-wall CNT content, while elongation decreased. Sharma et al. [81] studied the effect of the reinforcement incorporation approach on the mechanical, microstructure and tribological properties of AA6061-CNT nanocomposites fabricated by FSP. Multiple micro-sized channel reinforcement filling approach showed higher grain refinement than single micro-sized channel reinforcement filling approach. The distribution of CNT reinforcement particles in Al5083/CNT composites, after the third FSP pass is as shown in Figure 8.

### 3.12 Shape memory alloys and max phase materials

Along with the aforementioned reinforcement particles, shape memory alloys are also used as reinforcement for

MMCs fabrication. Shape memory alloys (SMAs) are metallic alloys that can regain their original shape after deformation occurs due to temperature and stress induced solid to solid phase transformation. NiTi, NiTiCu, CuAlNi, Cu-Zn-Al, and Fe-Mn-Si are preferred SMAs for most applications. Hartl et al. [83] described the properties and engineering effects of SMAs and discussed the aerospace application of SMAs. An introduction of SMAs into a light alloy matrix as a reinforcement to produce MMCs will provide low density, high strength, and a good shape memory effect. Ni et al. [84] fabricated Al6061/NiTi composites using friction stir processing and achieved the homogeneous distribution of NiTi<sub>p</sub> in the aluminium matrix without interfacial reaction. The prepared composites showed phase transformation behavior and enhanced strength. Figure 9a shows the morphology of NiTi particles. Huang et al. [85] found that NiTi<sub>p</sub> reinforcement in underwater FSP fabricated 5082Al-H112/NiTi composites can retain shape memory effect.

Recently, researchers used MAX phase materials as a reinforcement to fabricate metal matrix composites. The MAX phase materials are ternary layered compounds with the general formula  $M_{n+1}AX_n$  where  $M$  is a transition metal,  $A$  is an A group metal (IIIA and IVA in the periodic table) and  $X$  is C or N. These materials have combined properties of ceramics and metals. Good electrical conductivity, good machinability, thermal shock resistance, high strength and oxidation resistance make MAX phase materials to be of use in composite fabrication. Even though MAX phase materials are rarely explored as metal reinforcement, Ahmadifard et al. [86] have reinforced Ti<sub>3</sub>AlC<sub>2</sub> MAX phase particles into the Al7075 matrix by friction stir processing. Figure 9b shows the morphology of Ti<sub>3</sub>AlC<sub>2</sub> MAX phase particles. The composites fabricated by 4 passes of FSP showed enhanced microstructure, mechanical (19–20% improvement in yield and tensile strength, 33% increase in microhardness) and tribological properties. Because the time and temperature are minimal

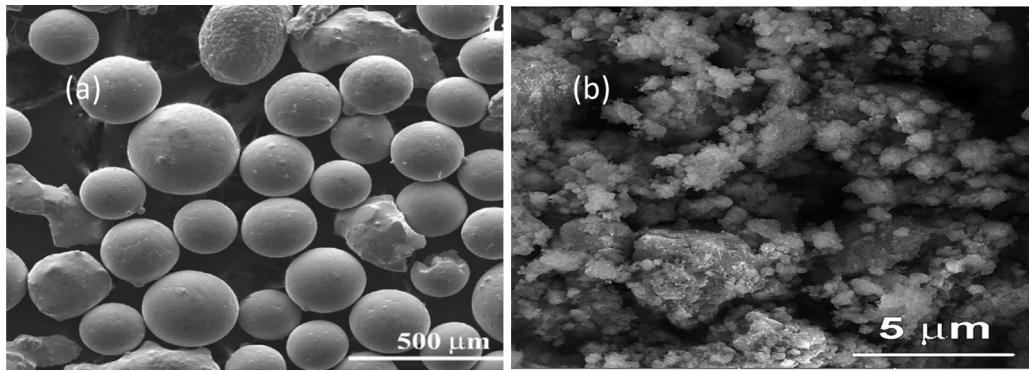


Fig. 9. Morphology of NiTiP and  $Ti_3AlC_2$  MAX powder [84,86].

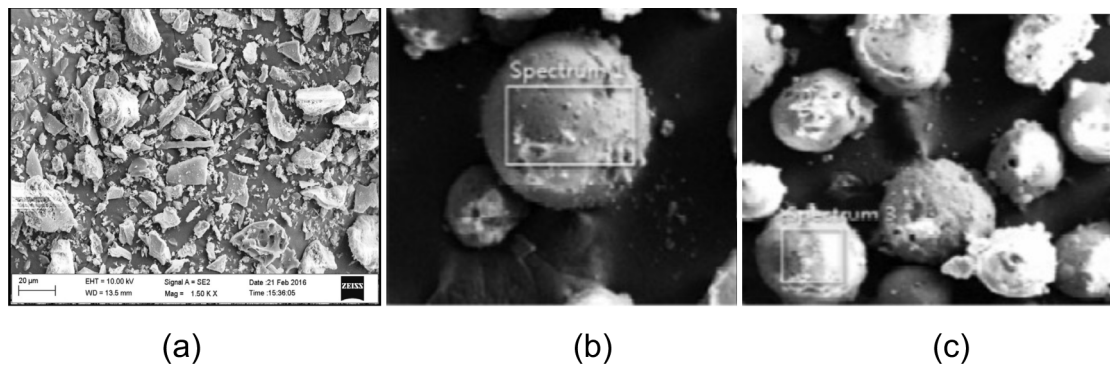


Fig. 10. SEM Micrographs of (a) RHA [90]; (b) Cenosphere fly ash; (c) Precipitator fly ash particles [96].

during FSP, there is less chance of an interaction between MAX Phase particles and the aluminium matrix. Ahmafidard et al. [87] observed that the FSP fabricated A356/ $Ti_3AlC_2$  surface composites with a high-volume fraction of  $Ti_3AlC_2$  particles showed maximum microhardness and tensile strength. A composite with a 7.5% volume fraction of particles was found to be richer in terms of microhardness (87 HV), tensile strength (184 MPa).

### 3.13 Industrial residue particles

Although incorporating hard ceramic particles into aluminium alloys improves the performance of composites, the higher cost of these particles raises the overall cost [88]. Low-priced and locally available materials are used as reinforcement to replace hard ceramic particles to bring down the cost. Researchers used industrial and agricultural wastes like Rice Husk Ash (RHA), fly ash (FA), red mud, coconut shell ash, eggshell ash, bamboo leaf ash, and bagasse ash as reinforcements. In addition to reducing costs, the use of these materials often reduces waste disposal issues.

#### 3.13.1 Rice husk ash particles

Rice Husk Ash (RHA) is available in large quantities, produced as an agricultural waste by-product. RHA is light in weight and contains SiC and  $Al_2O_3$  [89]. Dinaharan et al. [90] have fabricated Aluminium Matrix Composites

(AMC) by incorporating 18 Vol% of RHA into the AA6061 matrix and studied the microstructure and tensile behavior. SEM micrograph of RHA reinforcement particle used is as shown in Figure 10a. The author reported no agglomeration of RHA particles in composites and fine and equiaxed grain structures. RHA as reinforcement also improved microhardness in FSP fabricated AA7075/RHA surface composite by 11% more than base alloy [91].

#### 3.13.2 Fly ash particles

Fly ash materials are generated during coal combustion in thermal power plant and contain toxic contents. Fly ash particles are classified into two types, cenosphere and precipitator. Cenosphere are hollow fly ash particles with a density of less than 1.0 g/cc, and precipitators are solid fly ash particles with a density of 2–2.5 g/cc [92]. Figures 10b and 10c shows the SEM micrographs of cenosphere and precipitators fly ash particles respectively. Along with other composite fabrication techniques, researchers also took advantage of FSP to produce fly ash reinforced aluminium matrix composite [93,94]. Red mud is alkaline and contains heavy metals and other pollutants. Both fly ash and red mud are hazardous to the environment and pose a serious ecological issue. Using these by-products as reinforcement during composite preparation limits the disposal problem and enhances the material properties. Kumar et al. [88] used fly ash and red mud as reinforcement in the A356 alloy matrix to fabricate surface composite via FSP.

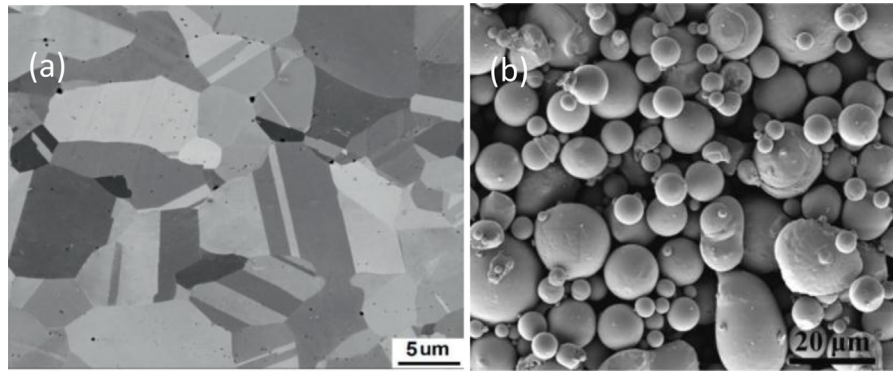


Fig. 11. SEM micrographs of CoCrFeNiMn [102]  $\text{Al}_{0.8}\text{CoCrFeNi}$  [101].

### 3.13.3 Rock dust particles

Rock dust is another naturally available material that contains higher silica content. Rock dust is easily available in stone-crushing plants as waste products and imposes a serious threat on human life if left out to atmospheric air. Dasari et al. [95] used rock dust as a reinforcement to incorporate in different weight % into the aluminium matrix using FSP. Author observed the improvement in wear resistance, impact strength, micro hardness but decreasing in elongation, yield strength and tensile strength than base metal matrix.

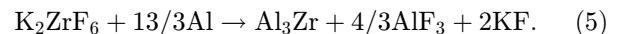
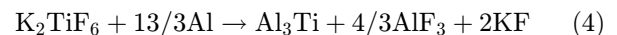
### 3.14 High entropy alloys

Another reinforcement used for the fabrication of metal matrix composite is high entropy alloys (HEA). HEAs are metallic alloys with more than five principal elements with equal or nearly equal molar fractions. AlCoCrFeNi, CoCrFeNi, FeCoNiCrAl and CrMnFeCoNi are commonly used HEA particles. To expose the use of HEAs as reinforcement in composite fabrication, Yang et al. [97] have incorporated AlCoCrFeNi particles into AA5083 alloy by submerged FSP method. The resulted AMC consist of equiaxed fine grains and improved yield strength and tensile strength. The multipass FSP leads to increased heat input and thereby interfacial reaction between aluminum matrix and particles. The introduction of a cooling medium during FSP can reduce the peak temperature and the thermal cycle gets shortened. While, Yazdipour et al. [98] used mixture of methanol and dry ice as cooling medium and applied behind the tool, Kumar et al. [99] conducted FSP operation in cryo environment to fabricate nanocomposite. FeCoNiCrAl high entropy alloy reinforced Al5083 composite fabricated by FSP technique, possessed higher microhardness and wear resistance [100]. The HEA particles have great potential to enhance conventional alloys' properties [101]. Figures 11a and (11)b shows the SEM micrographs of CoCrFeNiMn and  $\text{Al}_{0.8}\text{CoCrFeNi}$  particles respectively.

### 3.15 Intermetallics

Aluminum-rich intermetallics were used as reinforcement in the synthesis of AMMC due to issues of ceramic

particles.  $\text{Al}_3\text{Ti}$ ,  $\text{Al}_3\text{Zr}$ ,  $\text{Al}_3\text{Fe}$ ,  $\text{Al}_3\text{Ni}$ ,  $\text{Al}_3\text{Cu}$  are intermetallics used as reinforcement because of their low density, low coefficient of thermal expansion and high melting temperature. The intermetallics are formed by adding inorganic salt to molten aluminium. Hsu et al. [103] prepared Al-Cu, Al-Ti specimens from aluminium, copper and titanium powders. On application of FSP to Al-CU and Al-Ti specimens,  $\text{Al}_2\text{Cu}$  and  $\text{Al}_3\text{Ti}$  intermetallic phases were produced. Fotoohi et al. [104] prepared the reactive powder by mechanical alloying of Ni, Ti and C powders. The reactive powders were filled into channels created on the AA1050 alloy. FSP achieves the in-situ synthesis of  $\text{Al}_3\text{Ni}/\text{TiC}$  particles. Further, Dinaharan et al. [105] added inorganic salt  $\text{K}_2\text{TiF}_6$  or  $\text{K}_2\text{ZrF}_6$  into the molten aluminium, to form  $\text{Al}_3\text{Ti}$  or  $\text{Al}_3\text{Zr}$  intermetallics. AA6061/ $\text{Al}_3\text{Ti}$  and AA6061/ $\text{Al}_3\text{Zr}$  AMC are formed. These composites are then subjected to FSP, which enhanced the distribution and morphology of intermetallic particles. Equations (4) and (5) explain the formation of intermetallic phases.



### 3.16 Hybrid composites

Along with mono composites, researchers also developed hybrid composites to take advantage of different reinforcements. The combinations of reinforcements are incorporated into the metal matrix, and the effects of these hybrid mixtures on microstructural and mechanical behavior were studied. Yuvaraj et al. [106] have prepared mono and hybrid composites of Al5083 alloy by incorporating  $\text{B}_4\text{C}$  and TiC nanoparticles through FSP technique. Upon investigation, it was found that Al5083/ $\text{B}_4\text{C}/\text{TiC}$  surface nanocomposites have higher wear resistance (wear rate of 0.004 mg/m at 60 N sliding load). Narimani et al. [40] fabricated AA6063- $\text{B}_4\text{C}/\text{TiB}_2$  mono and hybrid composites by FSP and studied the microstructural and wear behavior. Both Boron carbide ( $\text{B}_4\text{C}$ ) and titanium diboride ( $\text{TiB}_2$ ) has excellent ballistic efficiency. The addition of these powder mixtures into AA7005 alloy to fabricate

**Table 3.** Work reported on composite fabrication via FSP.

Base material	Tool design parameters	Operating parameters	Reinforcement	Reinforcement technique	Remarks	References
AA5083	SD-16 mm PD-6 mm PL-3 mm	TR-800 rpm TS-50 mm/min	Al-Co-Cr-Fe-Ni series HEA powders	Blind holes	56% increase in hardness 42% increase in yield strength, 22% increase in UTS than FSPed base alloy	[101]
AA6061	SD-14 mm PD-5 mm, PL-2.7 mm	TR-1200 rpm WS-100 mm/min	B <sub>4</sub> C 5-7 μm	Groove	Improve wear resistance and microhardness	[31]
A356	SD-18 mm, PD-6 mm, PL=3.5 mm	TR-800, 1200, 1600 rpm WS-8, 32, 80 mm/min	B <sub>4</sub> C -10 μm	Groove	Higher rotational to traverse speeds ratio gives optimal properties.	[39]
Al5083	SD-18 mm, PD-6 mm, PL-4.5 mm	TR-800 rpm WS-35 mm/min	CeO <sub>2</sub> 50 nm, SiC 80 nm	Groove	The maximum hardness and tensile strength were obtained for the composite containing 100%SiC reinforcement	[59]
AA6063	SD-18 mm, PD-6 mm, PL-5.8 mm	TR-1000 rpm WS-30 mm/min	SiC	Groove	The high value of hardness	[112]
Al7075	SD-18 mm, PD 6-8 mm, PL-5.4 mm	TR-1200, 1400 rpm WS-30, 40 mm/min	SiC 30-40 μm	Groove	1.65-2.15 times increase in Hardness	[113]
AA6082	SD-16 mm, PD-5 mm, PL-4 mm	TR-1250 rpm, WS-135 mm/min	Al <sub>2</sub> O <sub>3</sub> 50 nm	Groove	An increase in FSP passes enhances hardness, wear resistance	[48]
AA6061	SD-27 mm, PD-10 mm, PL-3 mm	TR-480 rpm WS-203.2 mm/min	Al <sub>2</sub> O <sub>3</sub> 50 nm	Hole	The distribution of ceramic particles is more homogeneous as FSP passes increases.	[114]
AA2024	SD-25 mm PD-8 mm PL-2.5 mm	TR-900, 1120, 1400, 1800 rpm TS-10, 15, 20 mm/min	Al <sub>2</sub> O <sub>3</sub> 30 nm	Groove	A finer grain in second and third passes FSPed specimen, increase in ultimate tensile strength, hardness	[115]
AA6061	SD-12.5 mm, PD-5 mm, PL-2 mm	TR-1200 rpm WS-3 mm/s	Al <sub>2</sub> O <sub>3</sub> 320 nm, CNT 10-20 nm	Cylindrical holes	The presence of nano-sized reinforcement led to more pronounced grain refinement.	[50]
AA8026	SD-18 mm, PD-5 mm, PL-5 mm	TR-800, 1200, 1600 rpm WS-40, 80 mm/min	TiB <sub>2</sub> 5 μm Al <sub>2</sub> O <sub>3</sub> 70 nm	Groove	Type and size of reinforcement have an impact on mechanical properties	[116]
AA6082	SD-18 mm, PD-6 mm, PL-5.5 mm	TR-1600 rpm WS-60 mm/min	TiB <sub>2</sub> 20 μm BN- 200 nm	Groove	The addition of reinforcement enhances wear resistance.	[47]
Al7075	SD-24 mm, PD 6-8 mm	TR-1200 rpm WS-30 mm/min	TiC 3.5 μm	Groove	Increased hardness and corrosion resistance	[117]
AA1050	SD-15 mm, PD-3 mm, PL-3 mm	TR- 1000 rpm WS-20 mm/min	TiC 10 μm	Hole	Substantial improvement in microhardness, friction factor, wears resistance.	[118]
AA5052	SD-18 mm, PD-6 mm, PL-4.5 mm	TR-700, 1000, 1300 rpm WS-50, 65, 80 mm/min	TiO <sub>2</sub> 2 μm	Groove	Optimal process parameter for enhancement in mechanical properties.	[66]
Al3003	SD-18 mm, PD-3 mm, PL-4.3 mm	TR-1200 rpm WS-50 mm/min	TiO <sub>2</sub>	Groove	Grain refinement and 70% reduction in grain size	[69]
AA5083	SD-20 mm, PD-6 mm, PL-4.5 mm	TR-1600 rpm WS-60 mm/min	WC	Blind holes	Accelerated dynamic recrystallization on increasing vol. fraction and also enhanced strength and ductility	[25]
AA7075-T6	SD-18 mm PD-4 mm	TR-1200 rpm TS-20 mm/min	WC	Groove	9 wt% of WC nanoparticle addition improves metallurgical behavior in the matrix.	[119]

Table 3. (continued).

Base material	Tool design parameters	Operating parameters	Reinforcement	Reinforcement technique	Remarks	References
Al6061	SD-15 mm, PD-5 mm, PL-5.5 mm	TR-1200 rpm WS-50 mm/min	ZrB <sub>2</sub>	Direct melt reaction	Four pass FSP improves microstructural homogeneity	[64]
Al2024-T3	SD-20.32 mm, PD-9.53 mm, PL-8.89 mm	TR-400 rpm WS-355.6 mm/min	CNT and Al mixture	Groove	Unique dispersion of CNTs in four zones	[120]
Al5083	SD-16 mm, PD-4 mm	TR-880 rpm WS-25 mm/min	MWCNTs 150 nm	Side face groove	No agglomeration, grain size refined in composites, increase in tensile strength	[121]
AA6061	SD-18 mm, PD-6 mm, PL-5.7 mm	TR-1200 rpm TS-50 mm/min	Al <sub>3</sub> Fe (0-15 wt%)	Addition of iron powder into molten aluminium	Elimination of casting defects, improved tensile strength, removal of the sharp edge of Al <sub>3</sub> Fe particle	[122]

hybrid surface composite by FSP, improve the ballistic resistance [107]. Depth of penetration of the steel projectile on the 75B<sub>4</sub>C-25TiB<sub>2</sub> surface composite was 20 mm. Soleymani et al. [108] studied the microstructural and tribological properties of Al5083 surface hybrid composites produced using FSP. Al5083/SiC surface composite showed the highest hardness and Al5083/(SiC + MoS<sub>2</sub>) hybrid composite showed the highest wear resistance. Akbari et al. [109] used FSP technique to fabricate hybrid surface composite to improve the wear properties of Al-Si cast aluminium alloy A356. Jalilvand et al. [110] inserted Al<sub>2</sub>O<sub>3</sub> and SiO<sub>2</sub> particles into holes in the A356 alloy matrix and prepared surface hybrid nanocomposites using FSP. The fabricated composite showed uniform distribution of reinforcement particles, reduced porosity, and enhanced mechanical and corrosion properties. Sharma et al. [111] observed the rise in axial force at higher rotational speed, with graphite as reinforcement. The flaky nature and high thermal conductivity of graphite are responsible for this fluctuation. The authors successfully fabricated Al6061-SiC-Graphite hybrid composites by FSP and obtained optimized and uniform mechanical properties. Table 3 lists the different works reported on composite fabrication by FSP. In Table 3, the abbreviations used are; SD-shoulder diameter, PD-Pin diameter, PL-Pin length, TR-Tool rotation speed, and TS-welding speed.

#### 4 Future research scope

The preceding sections of this review article covered the different reinforcement particles used to fabricate AMMC by FSP. It has been established that the FSP is a cutting-edge innovative method for producing metal matrix and surface composites. The ability of FSP to produce component with superior mechanical, structural and functional properties widens the scope for usage of aluminium matrix composites in aviation, marine, automobile and other structural industries. There have been many developments in FSP since its inception to produce metal matrix and surface composites. There is still vast scope for FSP to develop AMMC with different reinforcement particles, which will enhance the mechanical, metallurgical and structural properties. Some of the future research scope of FSP in composite fabrication may be as follows:

- The major issue during composite fabrication via FSP is agglomeration of reinforcement particles. Even if the agglomeration problem can be solved by using suitable process parameters and reinforcement strategies (multi-pass FSP), uniform distribution of reinforcements in single pass FSP is still a cause for concern.
- The process of covering the powder filled groove or hole by a pin less FSP tool is time consuming. A new tooling design needs to be developed to eliminate the capping pass step. Additionally, it is also important to minimize the loss of reinforcement particles during FSP.
- Direct Friction Stir Processing (DFSP) tool method of introducing reinforcement particles during FSP has the great potential to replace groove or hole methods. The continuous hole within DFSP tool is used to introduce reinforcement particles into the metal matrix and

thereby eliminates the pre-FSP sample preparation work (machining and filling of groove/hole, capping pass) of groove/hole method. Further studies on DFSP method can bring it into dominance over other reinforcement strategies.

- Further investigation on In-Situ composites, hybrid composites fabrication by FSP can be grey area for future research.
- The utilization of piezoelectric ceramic powder as reinforcement and subsequent FSP can enhance the damping capacity of material. The capability of FSP to produce good structural material by using piezoelectric ceramic powder needs to be explored for larger interest.
- Future research should focus on the use of AMMC in biomedical applications that require materials which are both lightweight and biocompatible.
- More attention is needed on the usage of environment hazardous biowaste, mineral waste, industrial waste, scrap, agricultural waste as reinforcement materials to AMMC.
- The synthesis of surface composite over large surface area is hard to achieve by FSP technique, requiring further investigation.
- Even though lot of studies have been carried out to explore the use of FSP to fabricate aluminium metal matrix and surface composites at the laboratory level, few aspects like high tooling and processing cost of FSP is hindering the growth of FSP in industrial applications. So, efforts are needed to scale up the FSP to industrial applications.

## 5 Conclusions

The current article presented a review of different reinforcements used in the fabrication of aluminium matrix composites using FSP. Reinforcement particles may be preplaced over the aluminium base matrix, or strengthening phases were obtained from the in-situ reaction during material formation. The preplacing of particles over the matrix can be achieved through different methods. Groove and hole method are widely used preplacement methods. Ceramic, metallic and carbonaceous particles are successfully incorporated into the aluminium alloys using FSP. Numerous researchers have reported improvements in mechanical, microstructural and tribological properties of composites fabricated through FSP. In this review article, use of SiC, B<sub>4</sub>C, TiC, WC, TiB<sub>2</sub>, ZrB<sub>2</sub>, TiO<sub>2</sub>, CeO<sub>2</sub>, Al<sub>2</sub>O<sub>3</sub>, MoS<sub>2</sub> and CNT particles have been reported. Inclusion of hard ceramic particles SiC, TiC, B<sub>4</sub>C helped in enhancing strength and hardness of composites owing to their load bearing nature and activation of different strengthening mechanisms. The excellent ballistic efficiency parameters of TiB<sub>2</sub> particle helped in improving ballistic properties of composites along with hardness and wear properties. The solid lubricating nature of Al<sub>2</sub>O<sub>3</sub>, MoS<sub>2</sub>, BN forms tribo film and thereby improves tribological properties of composites. The cathodic inhibitor property of CeO<sub>2</sub> helped in fabricating aluminium composites with better resistance to pitting corrosion. Hybrid composites, which

are successfully manufactured through the FSP route, also showed property enhancement. Along with reinforcement type, size and volume fraction, other FSP variables like rotational tool speed, tool traverse speed, tool geometry, number of FSP pass and reinforcement strategy have a greater impact on the distribution of reinforcement particles.

Researchers explored the advanced engineering materials like high entropy alloys, shape memory alloys, MAX phase materials and intermetallics as reinforcement particles. Further, industrial and agricultural waste byproducts are also used as reinforcement to bring down the overall cost and to eliminate the disposal problem. The selection of reinforcement for composite fabrication is based on availability, application, cost, and optimum enhancement of properties.

The current review paper examines various reinforcing particles employed in the fabrication of surface composites using the FSP method. This will greatly assist researchers in selecting appropriate reinforcement particles for producing property-enhanced metal matrix composites. The article also encourages researchers to investigate high entropy alloys, shape memory alloys, MAX phase materials, and intermetallics as reinforcement particles, as scope for further research is observed and is gaining importance owing to their excellent compatibility with metal matrix, good interfacial bonding.

## References

1. M. Haghshenas, Metal-Matrix Composites. Reference Module in Materials Science and Materials Engineering (2016) 0–28
2. V. Sharma, Y. Gupta, B.V. Kumar, U. Prakash, V. Sharma, Y. Gupta et al., Friction stir processing strategies for uniform distribution of reinforcement in a surface composite friction stir processing strategies for uniform distribution of reinforcement in a surface composite, LMMP **31** (2015) 1384–1392
3. S. Rathee, S. Maheshwari, A.N. Siddiquee, Issues and strategies in composite fabrication via friction stir processing: a review, Mater. Manufactur. Process. **33** (2018) 239–261
4. O.M. Ikumapayi, E.T. Akinlabi, S.K. Pal, J.D. Majumdar, A survey on reinforcements used in friction stir processing of aluminium metal matrix and hybrid composites, Proc. Manufactur. **35** (2019) 935–940
5. V. Chak, H. Chattopadhyay, T.L. Dora, A review on fabrication methods, reinforcements and mechanical properties of aluminum matrix composites, J. Manufactur. Process. **56** (2020) 1059–1074
6. P. Samal, P.R. Vundavilli, A. Meher, M.M. Mahapatra, Recent progress in aluminium metal matrix composites: a review on processing, mechanical and wear properties, J. Manufactur. Process. **59** (2020) 131–152
7. P. Garg, A. Jamwal, D. Kumar, K.K. Sadasivuni, C.M. Hussain, P. Gupta, Advance research progresses in aluminium matrix composites: manufacturing & applications, J. Mater. Res. Technol. **8** (2019) 4924–4939
8. R.S. Mishra, M.W. Mahoney, S.X. McFadden, N.A. Mara, A.K. Mukherjee, High strain rate superplasticity in a friction stir processed 7075 Al alloy, Scr. Mater. **42** (1999) 163–168

9. G.K. Padhy, C.S. Wu, S. Gao, Friction stir based welding and processing technologies – processes, parameters, microstructures and applications: a review, *J. Mater. Sci. Technol.* **34** (2018) 1–38
10. R.S. Mishra, Z.Y. Ma, Friction stir welding and processing, *Mater. Sci. Eng. R: Rep.* **50** (2005) 1–78
11. K. Li, X. Liu, Y. Zhao, Research status and prospect of friction stir processing technology, *Coatings* **9** (2019) 1–14
12. S. Mironov, Y.S. Sato, H. Kokawa, Microstructural evolution during friction stir-processing of pure iron, *Acta Mater.* **56** (2008) 2602–2614
13. Z.Y. Ma, A.H. Feng, D.L. Chen, J. Shen, Recent advances in friction stir welding/processing of aluminum alloys: microstructural evolution and mechanical properties, *Crit. Rev. Solid State Mater. Sci.* **43** (2018) 269–333
14. V. Patel, W. Li, A. Vairis, V. Badheka, Recent development in friction stir processing as a solid-state grain refinement technique: microstructural evolution and property enhancement, *Crit. Rev. Solid State Mater. Sci.* **44** (2019) 378–426
15. V. Sharma, U. Prakash, B.V.M. Kumar, Surface composites by friction stir processing: a review, *J. Mater. Process. Technol.* **224** (2015) 117–134
16. B. Ratna Sunil, Different strategies of secondary phase incorporation into metallic sheets by friction stir processing in developing surface composites, *Int. J. Mech. Mater. Eng.* **11** (2016) 1–8
17. J. Iwaszko, M. Sajed, Technological aspects of producing surface composites by friction stir processing—a review, *J. Compos. Sci.* **5** (2021) 1–31
18. R.S. Mishra, Z.Y. Ma, I. Charit, Friction stir processing: a novel technique for fabrication of surface composite, *Mater. Sci. Eng. A* **341** (2003) 307–310
19. R. Srinivasu, A. Sambasiva Rao, G. Madhusudhan Reddy, K. Srinivasa Rao, Friction stir surfacing of cast A356 aluminium-silicon alloy with boron carbide and molybdenum disulphide powders, *Defence Technol.* **11** (2015) 140–146
20. H.G. Rana, V.J. Badheka, A. Kumar, Fabrication of Al7075/B<sub>4</sub>C surface composite by novel friction stir processing (FSP) and investigation on wear properties, *Proc. Technol.* **23** (2016) 519–528
21. E.R.I. Mahmoud, K. Ikeuchi, M. Takahashi, Fabrication of SiC particle reinforced composite on aluminium surface by friction stir processing, *Sci. Technol. Weld. Join.* **13** (2008) 607–618
22. C.M. Abreu, R. Acuña, M. Cabeza, M.J. Cristóbal, P. Merino, D. Verdura, Microstructure and mechanical properties of Al/SiC composite surface layer produced by friction stir processing, *Ciencia e Tecnol. Dos Mater.* **29** (2017) e82–e86
23. C. María Abreu Fernández, R.A. Rey, M. Julia Cristóbal Ortega, D. Verdura, C.L. Vidal, Friction stir processing strategies to develop a surface composite layer on AA6061-T6, *Mater. Manufactur. Process.* **33** (2018) 1133–1140
24. A. Thangarasu, N. Murugan, I. Dinaharan, S.J. Vijay, Microstructure and microhardness of AA1050/TiC surface composite fabricated using friction stir processing, *Sadhana – Acad. Proc. Eng. Sci.* **37** (2012) 579–586
25. G. Huang, W. Hou, Y. Shen, Evaluation of the microstructure and mechanical properties of WC particle reinforced aluminum matrix composites fabricated by friction stir processing, *Mater. Character.* **138** (2018) 26–37
26. A. Shafiei-Zarghani, S.F. Kashani-Bozorg, A. Zarei-Hanzaki, Microstructures and mechanical properties of Al/Al<sub>2</sub>O<sub>3</sub> surface nano-composite layer produced by friction stir processing, *Mater. Sci. Eng. A* **500** (2009) 84–91
27. H.C. Madhu, P. Ajay Kumar, C.S. Perugu, S.V. Kailas, Microstructure and mechanical properties of friction stir process derived Al-TiO<sub>2</sub> nanocomposite, *J. Mater. Eng. Perform.* **27** (2018) 1318–1326
28. M. Narimani, B. Lotfi, Z. Sadeghian, Investigating the microstructure and mechanical properties of Al-TiB<sub>2</sub> composite fabricated by Friction Stir Processing (FSP), *Mater. Sci. Eng. A* **673** (2016) 436–442
29. S. Bharti, N.D. Ghetiya, K.M. Patel, A review on manufacturing the surface composites by friction stir processing, *Mater. Manufactur. Process.* **36** (2021) 135–170
30. J. Selvam, Matrix and Reinforcement Materials for Metal Matrix Composites, Elsevier Ltd (2021) 1–27. <https://doi.org/10.1016/B978-0-12-803581-8.11890-9>
31. Y. Zhao, X. Huang, Q. Li, J. Huang, K. Yan, Effect of friction stir processing with B<sub>4</sub>C particles on the microstructure and mechanical properties of 6061 aluminum alloy, *Int. J. Adv. Manufactur. Technol.* **78** (2015) 1437–1443
32. N.A. El-Mahallawy, S.H. Zoalfakar, A. Abdel Ghaffar Abdel Maboud, Microstructure investigation, mechanical properties and wear behavior of Al 1050/SiC composites fabricated by friction stir processing (FSP), *Mater. Res. Express.* **6** (2019) 1–15
33. R.D. Bourkhani, A.R. Eivani, H.R. Nateghi, Through-thickness inhomogeneity in microstructure and tensile properties and tribological performance of friction stir processed AA1050-Al<sub>2</sub>O<sub>3</sub> nanocomposite, *Compos. B: Eng.* **174** (2019) 107061
34. S.M. Ma, P. Zhang, G. Ji, Z. Chen, G.A. Sun, S.Y. Zhong et al., Microstructure and mechanical properties of friction stir processed Al-Mg-Si alloys dispersion-strengthened by nano-sized TiB<sub>2</sub> particles, *J. Alloys Compd.* **616** (2014) 128–136
35. H. Rana, V. Badheka, A. Kumar, A. Satyaprasad, Strategical parametric investigation on manufacturing of Al-Mg-Zn-Cu alloy surface composites using FSP, *Mater. Manufactur. Process.* **33** (2018) 534–545
36. K.M. Mehta, V.J. Badheka, Wear behavior of boron-carbide reinforced aluminum surface composites fabricated by Friction Stir Processing, *Wear* **426–427** (2019) 975–980
37. M.C. Lorenzo-Martin, O.O. Ajayi, Surface layer modification of 6061 al alloy by friction stir processing and second phase hard particles for improved friction and wear performance, *J. Tribol.* **136** (2014) 1–6
38. M. Komarasamy, R.S. Mishra, J.A. Baumann, G. Grant, Y. Hovanski, Processing, microstructure and mechanical property correlation in Al-B<sub>4</sub>C surface composite produced via friction stir processing, *TMS Annu. Meet.* (2013) 39–46. <https://doi.org/10.1002/9781118658345.ch5>
39. M. Akbari, M.H. Shojaefard, P. Asadi, A. Khalkhali, Hybrid multi-objective optimization of microstructural and mechanical properties of B<sub>4</sub>C/A356 composites fabricated by FSP using TOPSIS and modified NSGA-II, *Trans. Nonferrous Metals Soc. China (English Edition)* **27** (2017) 2317–2333
40. M. Narimani, B. Lotfi, Z. Sadeghian, Evaluation of the microstructure and wear behaviour of AA6063-B<sub>4</sub>C/TiB<sub>2</sub> mono and hybrid composite layers produced by friction stir processing, *Surf. Coat. Technol.* **285** (2016) 1–10
41. E.T. Akinlabi, R.M. Mahamood, S.A. Akinlabi, E. Ogunmuyiwa, Processing parameters influence on wear resistance behaviour of friction stir processed Al-TiC composites, *Adv. Mater. Sci. Eng.* **2014** (2014) 1–13

42. I. Dinaharan, Influence of ceramic particulate type on microstructure and tensile strength of aluminum matrix composites produced using friction stir processing, *J. Asian Ceram. Soc.* **4** (2016) 209–218
43. A. Thangarasu, N. Murugan, Effect of ceramic particles on microstructure and mechanical properties of aluminium surface composite fabricated using friction stir processing, *Mater. Sci. Forum* **830–831** (2015) 440–443
44. K.O. Sanusi, E.T. Akinlabi, Friction-stir processing of a composite aluminium alloy (AA 1050) reinforced with titanium carbide powder, *Mater. Tehnolog.* **51** (2017) 427–435
45. D. Yadav, R. Bauri, Friction stir processing of Al-TiB<sub>2</sub> in situ composite: effect on particle distribution, microstructure and properties, *J. Mater. Eng. Perform.* **24** (2015) 1116–1124
46. R. Sharma, A.K. Singh, A. Arora, S. Pati, P.S. De, Effect of friction stir processing on corrosion of Al-TiB<sub>2</sub> based composite in 3.5 wt.% sodium chloride solution, *Trans. Nonferrous Metals Soc. China (English Edition)* **29** (2019) 1383–1392
47. R. Palanivel, I. Dinaharan, R.F. Laubscher, J.P. Davim, Influence of boron nitride nanoparticles on microstructure and wear behavior of AA6082/TiB<sub>2</sub> hybrid aluminum composites synthesized by friction stir processing, *Mater. Des.* **106** (2016) 195–204
48. A. Shafiei-Zarghani, S.F. Kashani-Bozorg, A.Z. Hanzaki, Wear assessment of Al/Al<sub>2</sub>O<sub>3</sub> nano-composite surface layer produced using friction stir processing, *Wear* **270** (2011) 403–412
49. N. Parumandla, K. Adepu, Effect of tool shoulder geometry on fabrication of Al/Al<sub>2</sub>O<sub>3</sub> surface nano composite by friction stir processing, *Particul. Sci. Technol.* **0** (2018) 1–10
50. Z. Du, M.J. Tan, J.F. Guo, G. Bi, J. Wei, Fabrication of a new Al-Al<sub>2</sub>O<sub>3</sub>-CNTs composite using friction stir processing (FSP), *Mater. Sci. Eng. A* **667** (2016) 125–131
51. H. Eftekharinia, A.A. Amadeh, A. Khodabandeh, M. Paidar, Microstructure and wear behavior of AA6061/SiC surface composite fabricated via friction stir processing with different pins and passes, *Rare Metals* **39** (2016) 1–7
52. K. Elangovan, V. Balasubramanian, Influences of tool pin profile and welding speed on the formation of friction stir processing zone in AA2219 aluminium alloy, *J. Mater. Process. Technol.* **200** (2008) 163–175
53. M.H. Shojaeefard, M. Akbari, Effect of tool pin profile on distribution of reinforcement particles during friction stir processing of B 4C / aluminum composites, *Proc. IMechE Part L* **0** (2016) 1–15
54. J. Tang, Y. Shen, J. Li, Investigation of microstructure and mechanical properties of SiC/Al surface composites fabricated by friction stir processing, *Mater. Res. Express* **6** (2019) 1–13
55. N. Gangil, S. Maheshwari, A.N. Siddiquee, Multipass FSP on AA6063-T6 Al: Strategy to fabricate surface composites, *Mater. Manufactur. Process.* **33** (2018) 805–811
56. S. Rathee, S. Maheshwari, A.N. Siddiquee, M. Srivastava, Effect of tool plunge depth on reinforcement particles distribution in surface composite fabrication via friction stir processing, *Defence Technol.* **13** (2017) 86–91
57. J. Tang, Y. Shen, J. Li, Influences of friction stir processing parameters on microstructure and mechanical properties of SiC/Al composites fabricated by multi-pin tool, *J. Manufactur. Process.* **38** (2019) 279–289
58. P. Vijayavel, V. Balasubramanian, S. Sundaram, Effect of shoulder diameter to pin diameter (D/d) ratio on tensile strength and ductility of friction stir processed LM25AA-5% SiCp metal matrix composites, *Mater. Des.* **57** (2014) 1–9
59. M. Amra, K. Ranjbar, R. Dehmolaei, Mechanical properties and corrosion behavior of CeO<sub>2</sub> and SiC incorporated Al5083 alloy surface composites, *J. Mater. Eng. Perform.* **24** (2015) 3169–3179
60. M.K. Gupta, Analysis of tribological behavior of Al/Gr/MoS<sub>2</sub> surface composite fabricated by friction stir process, *Carbon Lett.* **30** (2019) 399–408
61. N. Saini, C. Pandey, S. Thapliyal, D.K. Dwivedi, Mechanical properties and wear behavior of Zn and MoS<sub>2</sub> reinforced surface composite Al-Si alloys using friction stir processing, *Silicon* **10** (2018) 1979–1990
62. S.A. Alidokht, A. Abdollah-zadeh, S. Soleymani, H. Assadi, Microstructure and tribological performance of an aluminium alloy based hybrid composite produced by friction stir processing, *Mater. Des.* **32** (2011) 2727–2733
63. Z.Y. Zhang, R. Yang, Y. Li, G. Chen, Y.T. Zhao, M.P. Liu, Microstructural evolution and mechanical properties of friction stir processed ZrB<sub>2</sub>/6061Al nanocomposites, *J. Alloys Compd.* **762** (2018) 312–318
64. Z. Zhang, R. Yang, Y. Guo, G. Chen, Y. Lei, Y. Cheng et al. Microstructural evolution and mechanical properties of ZrB<sub>2</sub>/6061Al nanocomposites processed by multi-pass friction stir processing, *Mater. Sci. Eng. A* **689** (2017) 411–418
65. R. Prasad, S.P. Tewari, J.K. Singh, Microstructural and wear characterization of friction stir processed microstructural and wear characterization of friction stir processed ZrB<sub>2</sub>/AA7075 in-situ composites, *Mater. Res. Express.* **6** (2019) 1–14
66. V. Mathur, S.B. Prabu, G. Patel, A.K. Shettigar, Reinforcement of titanium dioxide nanoparticles in aluminium alloy AA 5052 through friction stir process, *Adv. Mater. Process. Technol.* **5** (2019) 329–337
67. V. Sharma, P. Tripathi, Approaches to measure volume fraction of surface composites fabricated by friction stir processing: a review, *Measurement* **193** (2022) 110941
68. F. Khodabakhshi, A. Simchi, A.H. Kokabi, M. Sadeghahmadi, A.P. Gerlich, Reactive friction stir processing of AA 5052-TiO<sub>2</sub> nanocomposite: process-microstructure-mechanical characteristics, *Mater. Sci. Technol.* **31** (2015) 426–435
69. K.A. Kumar, S. Natarajan, M. Duraiselvam, S. Ramachandra, Synthesis, characterization and mechanical behavior of Al 3003-TiO<sub>2</sub> surface composites through friction stir processing, *Mater. Manufactur. Process.* **34** (2019) 183–191
70. S. Ahmadifard, S. Kazemi, A. Momeni, A356/TiO<sub>2</sub> nanocomposite fabricated by friction stir processing: microstructure, mechanical properties and tribologic behavior, *Jom* **70** (2018) 2626–2635
71. V.K.S. Jain, J. Varghese, S. Muthukumar, Effect of first and second passes on microstructure and wear properties of titanium dioxide-reinforced aluminum surface composite via friction stir processing, *Arab. J. Sci. Eng.* **44** (2019) 949–957
72. G. Huang, J. Wu, W. Hou, Y. Shen, J. Gao, Producing of Al-WC surface composite by additive friction stir processing, *Mater. Manufactur. Process.* **34** (2019) 147–158
73. J. Rodelas, J. Lippold, Characterization of engineered nickel-base alloy surface layers produced by additive friction stir processing, *Metallogr. Microstruct. Anal.* **2** (2013) 1–12

74. B. Li, Y. Shen, L. Lei, W. Hu, Fabrication and evaluation of Ti 3Al p/Ti-6Al-4V surface layer via additive friction-stir processing, *Mater. Manufactur. Process.* **29** (2014) 412–417
75. A. Heidarpour, Fabrication and characterization of A5083-WC-Al<sub>2</sub>O<sub>3</sub> surface composite by friction stir processing, *J. Mater. Eng. Perform.* **28** (2019) 2747–2753
76. Z.Y. Liu, B.L. Xiao, W.G. Wang, Z.Y. Ma, Singly dispersed carbon nanotube/aluminum composites fabricated by powder metallurgy combined with friction stir processing, *Carbon* **50** (2012) 1843–1852
77. Z.Y. Liu, B.L. Xiao, W.G. Wang, Z.Y. Ma, Analysis of carbon nanotube shortening and composite strengthening in carbon nanotube/aluminum composites fabricated by multi-pass friction stir processing, *Carbon* **69** (2014) 264–274
78. Z. Du, M.J. Tan, J.F. Guo, J. Wei, Friction stir processing of Al-CNT composites, *Proc. Inst. Mech. Eng. L* **230** (2016) 825–833
79. H. Izadi, A.P. Gerlich, Distribution and stability of carbon nanotubes during multi-pass friction stir processing of carbon nanotube/aluminum composites, *Carbon* **50** (2012) 4744–4749
80. Q. Liu, L. Ke, F. Liu, C. Huang, L. Xing, Microstructure and mechanical property of multi-walled carbon nanotubes reinforced aluminum matrix composites fabricated by friction stir processing, *Mater. Des.* **45** (2013) 343–348
81. A. Sharma, H. Fujii, J. Paul, Influence of reinforcement incorporation approach on mechanical and tribological properties of AA6061-CNT nanocomposite fabricated via FSP, *J. Manufactur. Process.* **59** (2020) 604–620
82. S.A. Hosseini, K. Ranjbar, R. Dehmlaei, A.R. Amirani, Fabrication of Al5083 surface composites reinforced by CNTs and cerium oxide nano particles via friction stir processing, *J. Alloys Compd.* **622** (2015) 725–733
83. D.J. Hartl, D.C. Lagoudas, Aerospace applications of shape memory alloys, *Proc. Inst. Mech. Eng. G* **221** (2007) 535–552
84. D.R. Ni, J.J. Wang, Z.N. Zhou, Z.Y. Ma, Fabrication and mechanical properties of bulk NiTip/Al composites prepared by friction stir processing, *J. Alloys Compd.* **586** (2014) 368–374
85. G.Q. Huang, Y.F. Yan, J. Wu, Y.F. Shen, A.P. Gerlich, Microstructure and mechanical properties of fine-grained aluminum matrix composite reinforced with nitinol shape memory alloy particulates produced by underwater friction stir processing, *J. Alloys Compd.* **786** (2019) 257–271
86. S. Ahmadifard, A. Momeni, S. Bahmanzadeh, S. Kazemi, Microstructure, tribological and mechanical properties of Al7075 / Ti<sub>3</sub>AlC<sub>2</sub> MAX-phase surface composite produced by friction stir processing, *Vacuum* **155** (2018) 134–141
87. A. Manocherian, A. Heidarpour, Y. Mazaheri, S. Ghasemi, On the surface reinforcing of A356 aluminum alloy by nanolayered Ti<sub>3</sub>AlC<sub>2</sub> MAX phase via friction stir processing, *Surf. Coat. Technol.* **377** (2019) 124884
88. H. Kumar, R. Prasad, P. Kumar, S.P. Tewari, J.K. Singh, Mechanical and tribological characterization of industrial wastes reinforced aluminum alloy composites fabricated via friction stir processing, *J. Alloys Compd.* **831** (2020) 154832
89. M. Bilal, N. Shaikh, M. Ahmed, M. Zubair, A. Khan, Rice husk ash reinforced aluminium matrix composites: fabrication, characterization, statistical analysis and artificial neural network modelling Rice husk ash reinforced aluminium matrix composites: fabrication, characterization, analysis and artificial neural network modelling, *Mater. Res. Express* **6** (2019) 1–23
90. I. Dinaharan, K. Kalaiselvan, N. Murugan, Influence of rice husk ash particles on microstructure and tensile behavior of AA6061 aluminum matrix composites produced using friction stir processing, *Compos. Commun.* **3** (2017) 42–46
91. R. Butola, Q. Murtaza, Fabrication and optimization of AA7075 matrix surface composites using Taguchi technique via friction stir processing (FSP), *Eng. Res. Express* **1** (2019) 025015
92. A. Dey, K.M. Pandey, Characterization of fly ash and its reinforcement effect on metal matrix composites: a review, *Rev. Adv. Mater. Sci.* **44** (2016) 168–181
93. R. Nelson, I.S. Dinaharan, J. Vijay, Design and development of Fly ash reinforced aluminium matrix composite using friction stir process (FSP), in 2013 International Conference on Energy Efficient Technologies for Sustainability (2013), pp. 883–887
94. N.A. Patil, N. Zhongyan, S.R. Pedapati, O.B. Mamat, Investigation on effect of fly ash volume percentage on microstructure and microhardness of aa7075—fly ash surface composites via fsp, *Lect. Notes Mech. Eng.* (2020). [https://doi.org/10.1007/978-981-15-5753-8\\_37](https://doi.org/10.1007/978-981-15-5753-8_37)
95. S.N. Dasari, N.S. Potluri, A.V.S. Ramprasad, Influence of rock dust reinforcement on mechanical properties of Al composite using friction stir processing, *Austr. J. Mech. Eng.* **00** (2020) 1–10
96. A. Dey, K.M. Pandey, Characterization of fly ash and its reinforcement effect on metal matrix composites: a review, *Rev. Adv. Mater. Sci.* **44** (2016) 168–181
97. X. Yang, P. Dong, Z. Yan, B. Cheng, X. Zhai, AlCoCrFeNi high-entropy alloy particle reinforced 5083Al matrix composites with fine grain structure fabricated by submerged friction stir processing, *J. Alloys Compd.* **836** (2020) 155411
98. A. Yazdipour, M.A. Shafiei, K. Dehghani, Modeling the microstructural evolution and effect of cooling rate on the nanograins formed during the friction stir processing of Al5083, *Mater. Sci. Eng. A* **527** (2009) 192–197
99. A. Kumar, K. Pal, S. Mula, Effects of cryo-FSP on metallurgical and mechanical properties of stir cast Al7075-SiC nanocomposites, *J. Alloys Compd.* **852** (2021) 156925
100. J. Gao, X. Wang, S. Zhang, L. Yu, J. Zhang, Y. Shen, Producing of FeCoNiCrAl high-entropy alloy reinforced Al composites via friction stir processing technology, *Int. J. Adv. Manufactur. Technol.* **110** (2020) 569–580
101. J. Li, Y. Li, F. Wang, X. Meng, L. Wan, Z. Dong et al. Friction stir processing of high-entropy alloy reinforced aluminum matrix composites for mechanical properties enhancement, *Mater. Sci. Eng. A* **792** (2020) 139755
102. D. Shaysultanov, N. Stepanov, S. Malopheyev, I. Vysotskiy, V. Sanin, S. Mironov, Materials characterization friction stir welding of a carbon-doped CoCrFeNiMn high-entropy alloy, *Mater. Characteriz.* **145** (2018) 353–361
103. C.J. Hsu, P.W. Kao, N.J. Ho, Intermetallic-reinforced aluminum matrix composites produced in situ by friction stir processing, *Mater. Lett.* **61** (2007) 1315–1318
104. H. Fotoohi, B. Lotfi, Z. Sadeghian, J. Byeon, Microstructural characterization and properties of in situ Al-Al 3 Ni/TiC hybrid composite fabricated by friction stir processing using reactive powder, *Mater. Characteriz.* **149** (2019) 124–132

105. I. Dinaharan, Ashok G. Kumar, S.J. Vijay, N. Murugan, Development of  $Al_3Ti$  and  $Al_3Zr$  intermetallic particulate reinforced aluminum alloy AA6061 in situ composites using friction stir processing, *Mater. Des.* **63** (2014) 213–222
106. N. Yuvaraj, S. Aravindan Vipin, Wear characteristics of Al5083 surface hybrid nano-composites by friction stir processing, *Trans. Indian Inst. Metals* **70** (2017) 1111–1129
107. N. Pol, G. Verma, R.P. Pandey, T. Shanmugasundaram, Fabrication of AA7005/ $TiB_2$ - $B_4C$  surface composite by friction stir processing: evaluation of ballistic behaviour, *Defence Technol.* **15** (2019) 363–368
108. S. Soleymani, A. Abdollah-zadeh, S.A. Alidokht, Microstructural and tribological properties of Al5083 based surface hybrid composite produced by friction stir processing, *Wear* **278–279** (2012) 41–47
109. M. Akbari, M.H. Shojaeefard, P. Asadi, A. Khalkhali, Wear and mechanical properties of surface hybrid metal matrix composites on Al-Si aluminum alloys fabricated by friction stir processing, *Proc. Inst. Mech. Eng. L* **233** (2019) 790–799
110. Y.M. Jalilvanda Mohammad Mahdi, M.R. Akbar Heidar-pourb, Development of A356/ $Al_2O_3 + SiO_2$  surface hybrid nanocomposite by friction stir processing, *Surf. Coat. Technol.* **360** (2019) 121–132
111. A. Sharma, V. Sharma, S. Mewar, S. Pal, J. Paul, Friction stir processing of Al6061-SiC-graphite hybrid surface composites, *Mater. Manufactur. Process.* **33** (2018) 795–804
112. Rajesh, P. Kaushik, Micro structural behavior analysis of friction stir processed Al alloy AA6063/SiC, *Int. J. Mech. Eng. Technol.* **8** (2017) 991–998
113. R. Ande, P. Gulati, D.K. Shukla, H. Dhingra, ScienceDirect microstructural and wear characteristics of friction stir processed Al-7075/SiC reinforced aluminium composite, *Mater. Today* **18** (2019) 4092–4101
114. M. Yang, C. Xu, C. Wu, K.C. Lin, Y.J. Chao, L. An, Fabrication of AA6061/ $Al_2O_3$  nano ceramic particle reinforced composite coating by using friction stir processing, *J. Mater. Sci.* **45** (2010) 4431–4438
115. E. Moustafa, Effect of multi-pass friction stir processing on mechanical properties for AA2024/ $Al_2O_3$  nanocomposites, *Materials* **10** (2017) 1–17
116. H. Eskandari, R. Taheri, F. Khodabakhshi, Friction-stir processing of an AA8026- $TiB_2$ - $Al_2O_3$  hybrid nanocomposite: microstructural developments and mechanical properties, *Mater. Sci. Eng. A* **660** (2016) 84–96
117. S. Kumar, A. Kumar, C. Vanitha, Corrosion behaviour of Al 7075 /TiC composites processed through friction stir processing, *Mater. Today: Proc.* **15** (2019) 21–29
118. A. Shiva, M. Cheepu, V.C. Kantumuchu, K. Ravi Kumar, D. Venkateswarlu, B. Srinivas et al., Microstructure characterization of Al-TiC surface composite fabricated by friction stir processing, *IOP Conf. Ser.: Mater. Sci. Eng.* **330** (2018) 1–10
119. L.F. Ali, R. Soundararajan, S. Jeyasurya, M. Kovarthanam, S.N. Prasath, Materials Today: Proceedings Metallurgical assessment of AA7075-T6 with x wt % tungsten carbide nanoparticle surface composites processed by FSP route, *Mater. Today: Proc.* **45** (2020) 2152–2158
120. H.E. Misak, C.A. Widener, D.A. Burford, R. Asmatulu, Fabrication and characterization of carbon nanotube nanocomposites into 2024-T3 Al substrates via friction stir welding process, *J. Eng. Mater. Technol. Trans. ASME* **136** (2014) 1–5
121. T. Owa, Y. Shimizu, Fabrication and strength behavior of MWCNT-reinforced 5083 aluminum alloy composite via friction stir processing, *Mater. Trans.* **59** (2018) 1798–1804
122. M. Balakrishnan, I. Dinaharan, R. Palanivel, R. Sathiskumar, Effect of friction stir processing on microstructure and tensile behavior of AA6061/ $Al_3Fe$  cast aluminum matrix composites, *J. Alloys Compd.* **785** (2019) 531–541

**Cite this article as:** Karthik Adiga, Mervin A. Herbert, Shrikantha S. Rao, Arunkumar Shettigar, Applications of reinforcement particles in the fabrication of Aluminium Metal Matrix Composites by Friction Stir Processing - A Review, *Manufacturing Rev.* **9**, 26 (2022)